AVR435: BLDC/BLAC Motor Control Using a Sinus Modulated PWM Algorithm

8-bit AVR® Microcontrollers

Application Note

1. Features

- Cost-effective and energy efficient BLDC/BLAC motor drive
- Implemented on an AT90PWM3 AVR® low cost microcontroller
- Low memory and computing requirements

2. Introduction

Equipped with Hall effect sensors, permanent magnet motors are generally powered by currents of 'trapezoidal' shape (Figure 2-1a). In order to improve the system's performance (less noise, less torque ripple) it can be an advantage to power these motors using currents that have a 'sinusoidal' form (Figure 2-1b). BLDC motors are designed to be supplied with a trapezoidal shape current, respectively BLAC motors are designed to be supplied with a sinusoidal shape current, This application note proposes an implementation using the latter with an ATAVRMC100 board mounted with an AT90PWM3B.

Figure 2-1. 3 Phases Output Voltages vs Hall Sensor Inputs

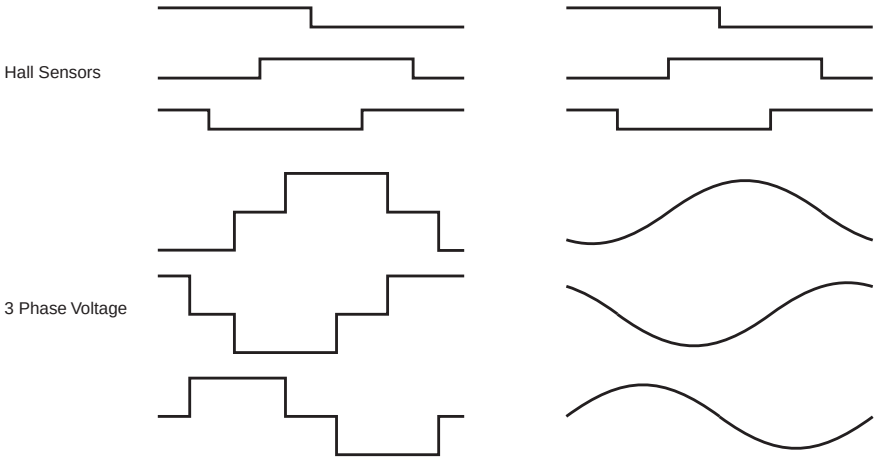

7671A–AVR–09/06

3. AT90PWM3B Key Features

The control algorithms have been implemented on the AT90PWM3B, a low-cost low-power single-chip microcontroller, achieving up to 16 MIPS and suitable for the control of DC-DC buck-boost converters, permanent magnet synchronous machines, three-phase induction motors and brushless DC motors. This device integrates:

- **8-bit AVR advanced RISC architecture microcontroller (core similar to the ATmega 88)**
- **8K Bytes of In-System-Programmable Flash memory**
- **512 Bytes of static RAM to store variables and lookup tables dedicated to the application program**
- **512 bytes of EEPROM to store configuration data and look-up tables**
- **one 8-bit timer and one 16-bit timer**
- **6 PWM channels optimized for Half-Bridge Power Control with 64MHz PLL Clock**
- **an 11-channel 10-bit ADC and a 10-bit DAC**
- **3 on-chip comparators**
- **a programmable watchdog timer with an internal oscillator**

4. Theory of Operation

4.1 Introduction

This implementation is based on the use of the Space-Vector Modutation (SVPWM) technique. The different sectors are determined and synchronized with the Hall sensors.

4.2 Principle of the Space-Vector Modulation

Figure 4-1. Typical structure of the application.

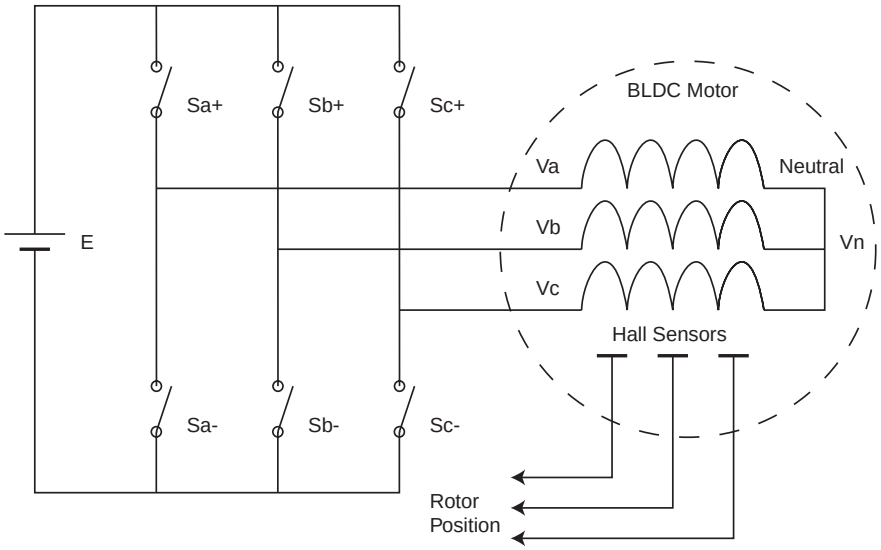

Figure 4-1 shows the typical structure of a BLDC/BLAC motor connected to a Voltage Source Inverter. Since the motor is considered as a balanced load with an unconnected neutral,

$$V_n = \langle V_a + V_b + V_c \rangle / 3 ,$$
$$V_{an} = V_a - V_n = (V_{ab} - V_{ca})/3 ,$$
$$V_{bn} = V_b - V_n = (V_{bc} - V_{ab})/3$$

and $$V_{cn} = V_c - V_n = (V_{ca} - V_{bc})/3 .$$

Since the upper power switches can only be On or Off, and since the lower ones are supposed to always be in the opposed state (the dead-times of the inverter legs are neglected), there are only eight possible switching states, as shown on Table 4-2. Six of them lead to non-zero phase voltages, and two interchangeable states lead to zero phase voltages. When mapped in a 2D-frame fixed to the stator using a Concordia transformation [1,2], the six non-zero phase voltages form the vertices of a hexagon. (See Figure 4-3)

$$\begin{bmatrix} V_\alpha \\ V_\beta \end{bmatrix} = \begin{bmatrix} 1 & -\frac{1}{2} & -\frac{1}{2} \\ 0 & \frac{\sqrt{3}}{2} & -\frac{\sqrt{3}}{2} \end{bmatrix} \times \begin{bmatrix} V_{an} \\ V_{bn} \\ V_{cn} \end{bmatrix}$$

Figure 4-2. Possible switching configurations of a 3-phase inverter

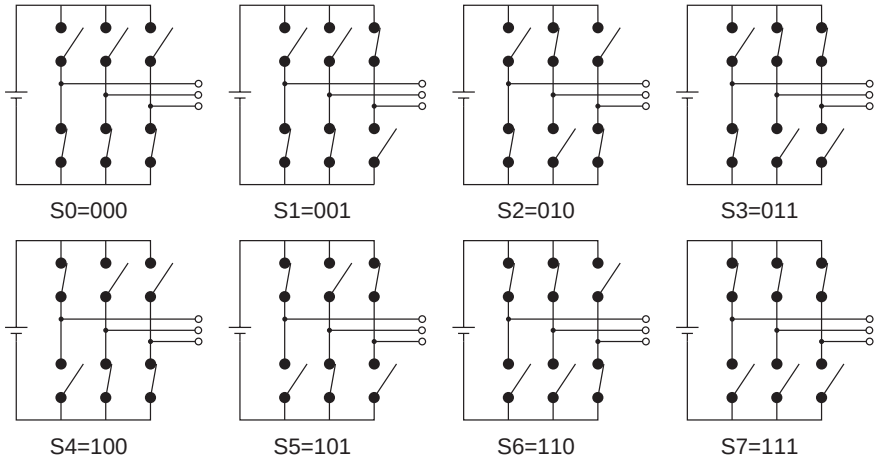

As shown on Figure 4-3, the angle between two successive non-zero voltages is always 60 degrees.

In complex form, these non-zero phase voltages can be written as $V_k = E e^{j(k-1)\frac{\pi}{3}}$, with *k* = 1..6 and $V_0 = V_7 = 0$ V.
Table 4-1 shows the line-to-line and line-to-neutral voltages in each of the 8 possible configurations of the inverter.

Figure 4-3. Representation of the eight possible switching configurations in the Concordia reference frame

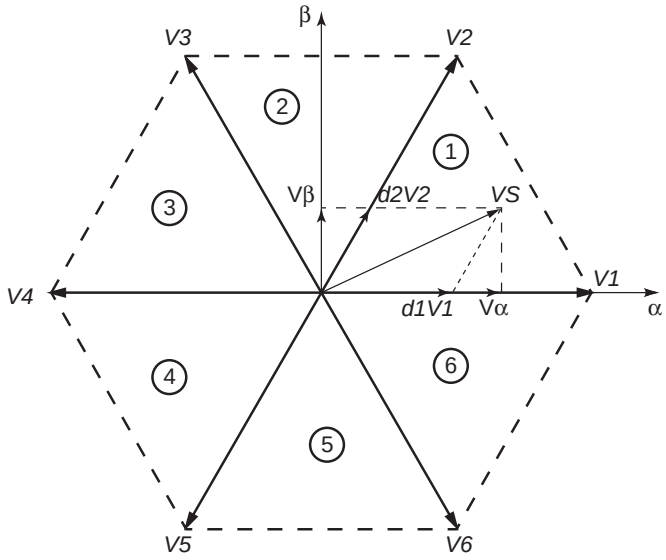

Table 4-1. Switching configurations and output voltages of a 3-phase inverter

S_{a+}	S_{b+}	S_{c+}	S_i	V_{ab}	V_{bc}	V_{ca}	V_{an}	V_{bn}	V_{cn}	V_α	V_β	V_i
0	0	0	S_0	0	0	0	0	0	0	0	0	V_0
0	0	1	S_1	0	-E	E	-E/3	-E/3	+2E/3	-E/2	$-E\sqrt{3}/2$	V_5
0	1	0	S_2	-E	E	0	-E/3	+2E/3	-E/3	-E/2	$E\sqrt{3}/2$	V_3

Table 4-1. Switching configurations and output voltages of a 3-phase inverter

S_{a+}	S_{b+}	S_{c+}	S_i	V_{ab}	V_{bc}	V_{ca}	V_{an}	V_{bn}	V_{cn}	V_α	V_β	V_i
0	1	1	S_3	-E	0	E	-2E/3	-E/3	-E/3	-E	0	V_4
1	0	0	S_4	E	0	-E	+2E/3	-E/3	-E/3	E	0	V_1
1	0	1	S_5	E	-E	0	E/3	-2E/3	E/3	E/2	$-E\sqrt{3}/2$	V_6
1	1	0	S_6	0	E	-E	E/3	E/3	-2E/3	E/2	$E\sqrt{3}/2$	V_2
1	1	1	S_7	0	0	0	0	0	0	0	0	V_7

Table 4-2. Expressions of the duty cycles in each sector

Sector Number	θ	d_k	d_{k+1}
1	$[0,\frac{\pi}{3}]$	$\frac{2}{\sqrt{3}}\times\frac{V_S}{E}\times\sin\langle\frac{\pi}{3}-\theta\rangle$	$\frac{2}{\sqrt{3}}\times\frac{V_S}{E}\times\sin\langle\theta\rangle$
2	$[\frac{\pi}{3},\frac{2\pi}{3}]$	$\frac{2}{\sqrt{3}}\times\frac{V_S}{E}\times\sin\langle\frac{\pi}{3}+\theta\rangle$	$\frac{2}{\sqrt{3}}\times\frac{V_S}{E}\times\sin\langle\frac{5\pi}{3}+\theta\rangle$
3	$[\frac{2\pi}{3},\pi]$	$\frac{2}{\sqrt{3}}\times\frac{V_S}{E}\times\sin\langle\theta\rangle$	$\frac{2}{\sqrt{3}}\times\frac{V_S}{E}\times\sin\langle\frac{4\pi}{3}+\theta\rangle$
4	$[\pi,\frac{4\pi}{3}]$	$\frac{2}{\sqrt{3}}\times\frac{V_S}{E}\times\sin\langle\frac{5\pi}{3}+\theta\rangle$	$\frac{2}{\sqrt{3}}\times\frac{V_S}{E}\times\sin\langle2\pi-\theta\rangle$
5	$[\frac{4\pi}{3},\frac{5\pi}{3}]$	$\frac{2}{\sqrt{3}}\times\frac{V_S}{E}\times\sin\langle\frac{4\pi}{3}+\theta\rangle$	$\frac{2}{\sqrt{3}}\times\frac{V_S}{E}\times\sin\langle\frac{\pi}{3}-\theta\rangle$
6	$[\frac{5\pi}{3},2\pi]$	$\frac{2}{\sqrt{3}}\times\frac{V_S}{E}\times\sin\langle2\pi-\theta\rangle$	$\frac{2}{\sqrt{3}}\times\frac{V_S}{E}\times\sin\langle\frac{\pi}{3}+\theta\rangle$

In the Concordia frame, any stator voltage $V_s = V_\alpha + jV_\beta = V_{sm}\cos(\theta) + jV_{sm}\sin(\theta)$ located inside this hexagon belongs to one of the six sectors, and can be expressed as a linear combination of the two non-zero phase voltages which delimit this sector: $V_s = d_k V_k + d_{k+1}V_{k+1}$. Equating $d_k V_k + d_{k+1}V_{k+1}$ to $V_{sm}\cos(\theta) + jV_{sm}\sin(\theta)$ in each sector leads to the expressions of the duty cycles shown in Table 4-2 Since the inverter cannot instantaneously generate V_s, the space-vector PWM principle consists in producing a T_s-periodic voltage whose average value equals V_s,by generating V_k during $T_k = d_k T_s$ and V_{k+1} during $T_{k+1} = d_{k+1}T_s$. Since $d_k + d_{k+1} \le 1$, these voltages must be completed over the switching period T_s by V_0 and/or V_7. Several solutions are possible, and the one which minimizes the total harmonic distorsion of the stator current consists in applying V_0 and V_7 during the same duration $T_0 = T_7 = \frac{1 - d_k - d_{k+1}}{2}T_s$. V_0 is equally applied at the beginning and at the end of the switching period, whereas V_7 is applied at the middle. As an illustration, the upper side of Figure 4-4 shows the waveforms obtained in sector 1.

4.3 Efficient Implementation of the SV-PWM

Table 4-2 seems to show that the duty cycles have different expressions in each sector. A thorough study of these expressions show that since $\sin(x) = \sin(\pi - x)$, all these duty cycles can be written in a unified way as $d_k = \frac{2V_{sm}}{E\sqrt{3}}\sin(\theta'')$ and $d_{k+1} = \frac{2V_{sm}}{E\sqrt{3}}\sin(\theta')$, with $\theta'' = \frac{\pi}{3} - \theta'$ and $\theta' = \theta - (k-1)\frac{\pi}{3}$. Since these expressions no longer depend on the sector number, they can be denoted as d_a and d_b. Since θ' is always between 0 and $\frac{\pi}{3}$, computing d_a and d_b requires a sine table for angles inside this interval only. This greatly reduces the amount of memory required to store this sine table.

The AT90PWM3 provides the 3 power stage controllers (PSC) needed to generate the switching waveforms computed from the Space Vector algorythms.

The counters will count from zero to a value corresponding to one half of the switching period (as shown on the lower side of Fig. 4), and then count down to zero. The values that must be stored in the three compare registers are given in Table 4-3

Figure 4-4. Inverter switch waveforms and corresponding compare register values

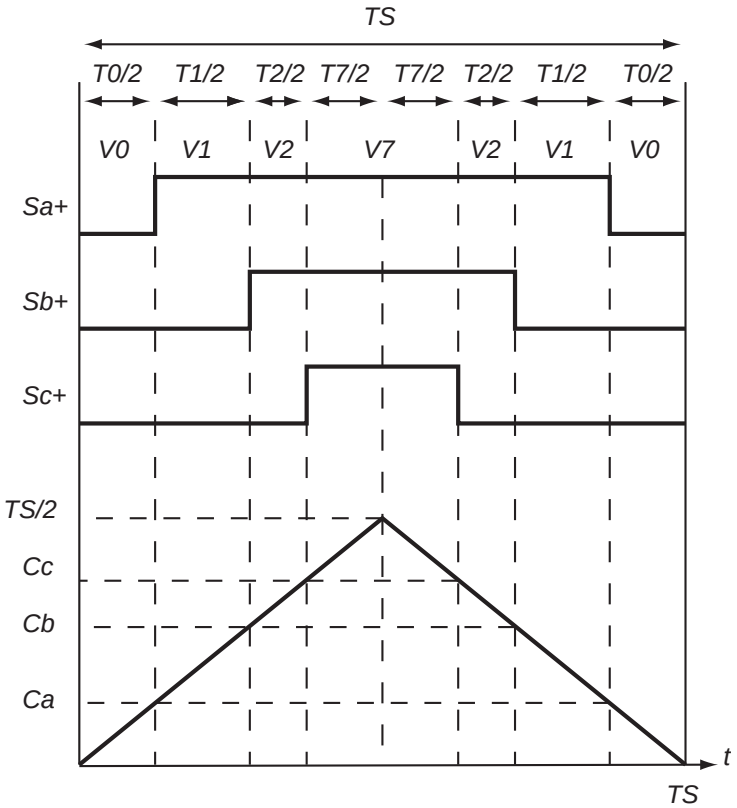

Table 4-3. Compare Register Values vs Sector Number

Sector Number	$\frac{4}{T_s}C_a - 1$	$\frac{4}{T_s}C_b - 1$	$\frac{4}{T_s}C_c - 1$
1	$-d_a - d_b$	$d_a - d_b$	$d_a + d_b$
2	$-d_a + d_b$	$-d_a - d_b$	$d_a + d_b$
3	$d_a + d_b$	$-d_a - d_b$	$d_a - d_b$
4	$d_a + d_b$	$-d_a + d_b$	$-d_a - d_b$
5	$d_a - d_b$	$d_a + d_b$	$-d_a - d_b$
6	$-d_a - d_b$	$d_a + d_b$	$-d_a + d_b$

4.4 Sector Determination Algorithm

The Sector Determination is based on the reading of the three Hall sensors. All along one electrical revolution, the three Hall sensors generates 6 steps. These 6 steps divide the circle in 6 sectors which will be used in the SVPWM (see Figure 4-5)

Figure 4-5. Sector Determination

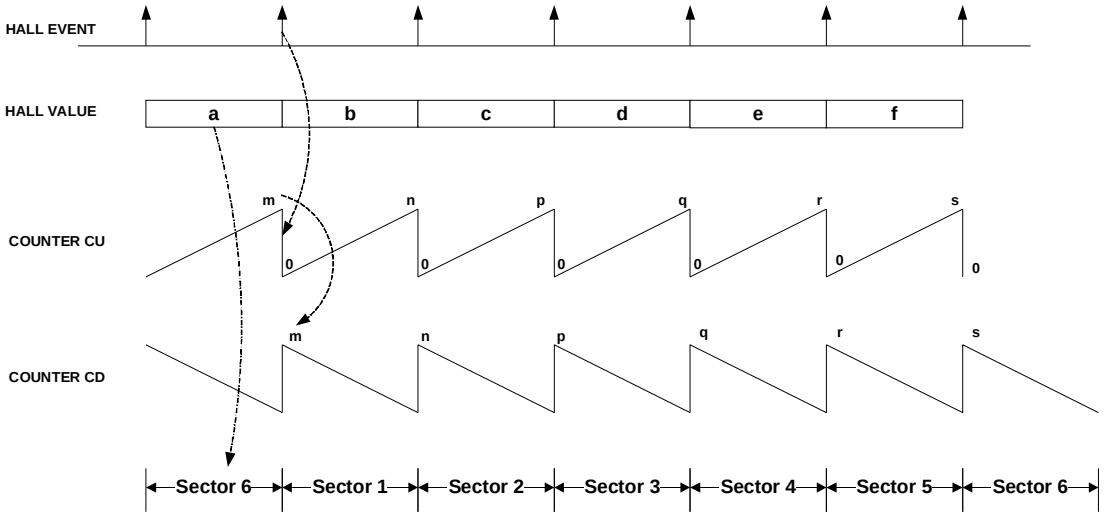

Inside one sector a counter, CU is incremented at a rate given by a high frequency reference clock. At the end of the sector the counter CU is copied into the counter CD. Then this counter CD is decremented by the same reference rate. This counter CD reflects the value of the angle ϑ of V_S vector inside a sector (see Figure 4-6) For example during sector 1, counter CU is incremented from 0 to n. At Hall Event, counter CU is copied in counter CD. Then during sector 2 counter CU is incremented and counter CD is decremented. Counter CD will drive the rotation of the vector Vs (see Figure 4-6)

Figure 4-6. Rotation of V_s Vector

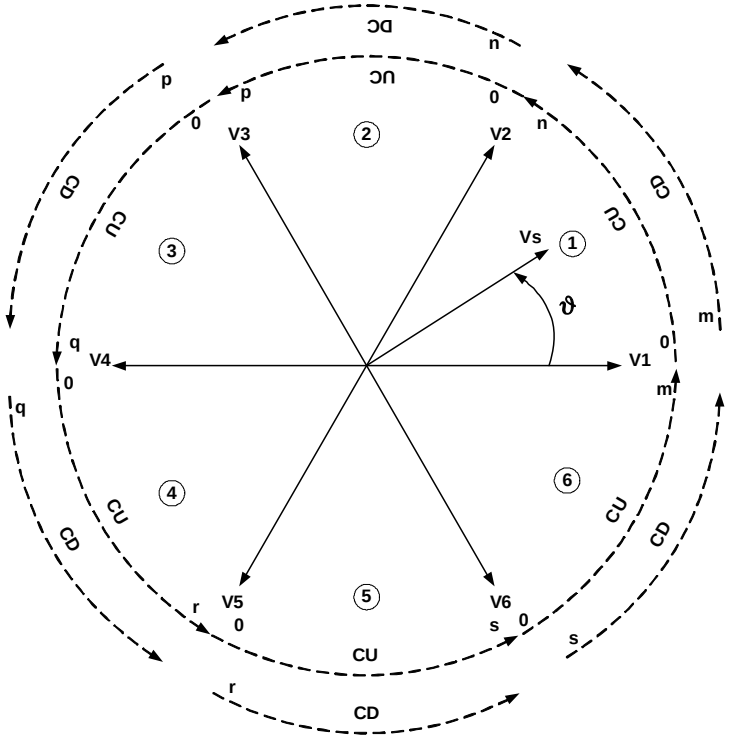

Figure 4-7 shows the data flow of the implementation of this SVPWM core. The Hall Sensors gives the sector number and the two angles ϑ‘ and ϑ‘‘. These angles point in a sine table. The sine value is multiplied by the voltage to calculate da and db. Then d_a and d_b are used to determine the compare values sent to the PSC (see Figure 4-4 on page 6).

Figure 4-7. Space Vector PWM data flow diagram

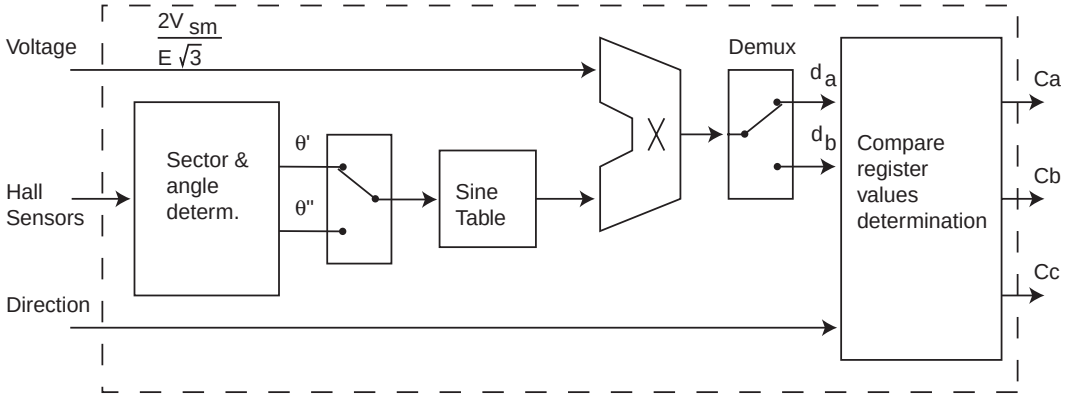

The resulting dataflow diagram, shown on Figure 4-7, can be used to build a speed control loop (Figure 4-8), in which the difference between the desired speed and the measured speed feeds a PI controller that determines the stator voltage frequency.

Figure 4-8. Block diagram of the complete control system.

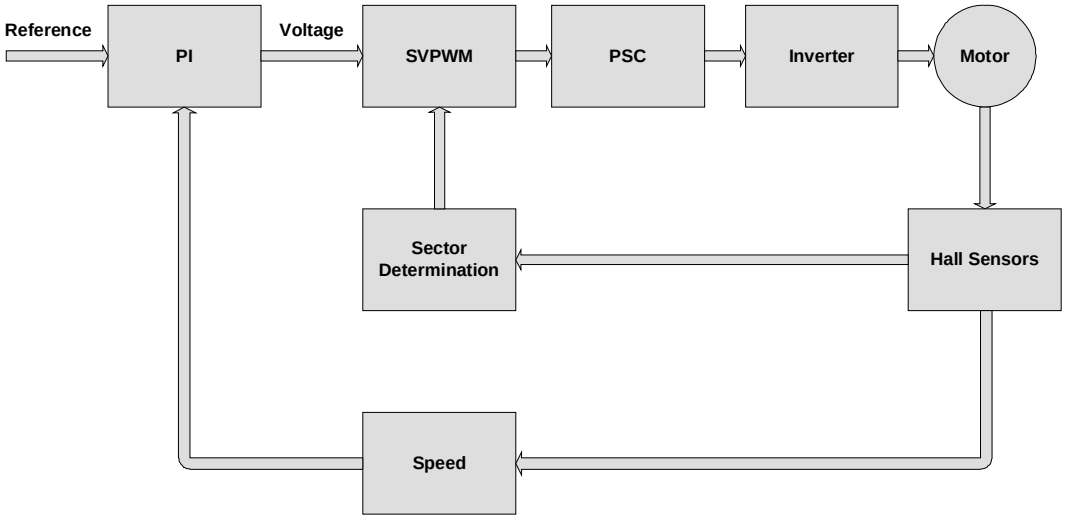

5. Hardware Description (ATAVRMC100)

This application is available on the ATAVRMC100 evaluation board equipped with an AT90PWM3B. This board provides a way to start and experiment BLDC and BLAC motor control.

ATAVRMC100 main features:

- AT90PWM3 microcontroller
- 12VDC motor drive
- ISP & Emulator interface

6. Software Description

All algorithms have been written in the C language using IAR Embedded Workbench® and AVR Studio® as development tools. For the space vector PWM algorithm, a table of the rounded values of $127\sin(\frac{2\pi k}{480})$ for k between 0 and 80 is used. The length of this table (81 bytes) is a better trade-off between the size of the available internal memory and the quantification of the rotor shaft speed. For bi-directional speed control, the values stored in two of the comparators are interchanged when the output of the PI regulator is a negative number (see Figure 4-8).

6.1 Project Description

The software is available in the attached project on the Atmel web Site.

An html documentation is included in the package. Use the index.html file in the doc directory to start viewing this documentation.

6.2 Resources

This values include all the application ressources (main, serial communication...)

Code Size : 4 408bytes

RAM Size : 291 bytes

CPU Load : 33% @ 16MHz

Timer 0 is used for speed measurement/main tick/svpwm

Timer 1 is not used

PSC0,1,2 are used to generate PWM

ADC is used for current measurement. It is synchronized by PSC on the PWM waveform.

6.3 Experimentation

Figure 6-1 shows the voltage between one phase and neutral point obtained with the microcontroller for speed reference 7000 rpm. Figure 6-2 shows the voltage between two phases obtained with the microcontroller for speed reference 7000 rpm.These experimental results were obtained with the BLDC motor included in the kit.

Figure 6-1. Voltage between one phase and neutral point @7000rpm

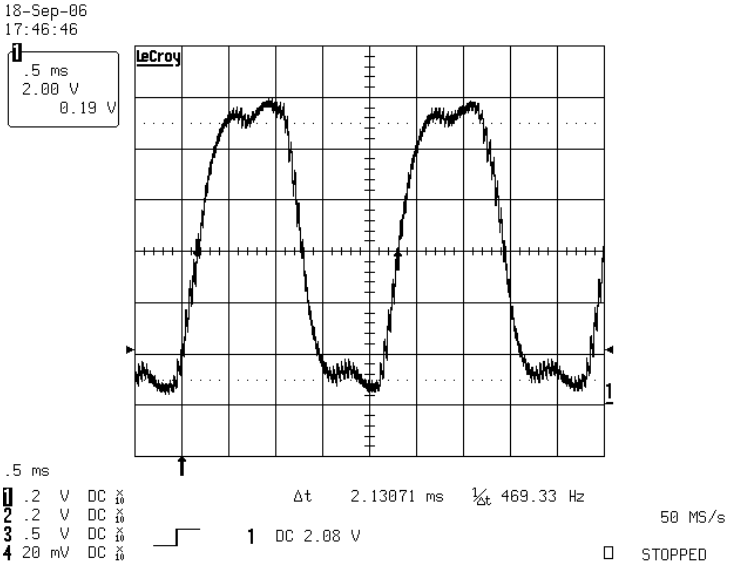

Figure 6-2. Voltage between two phases @7000rpm

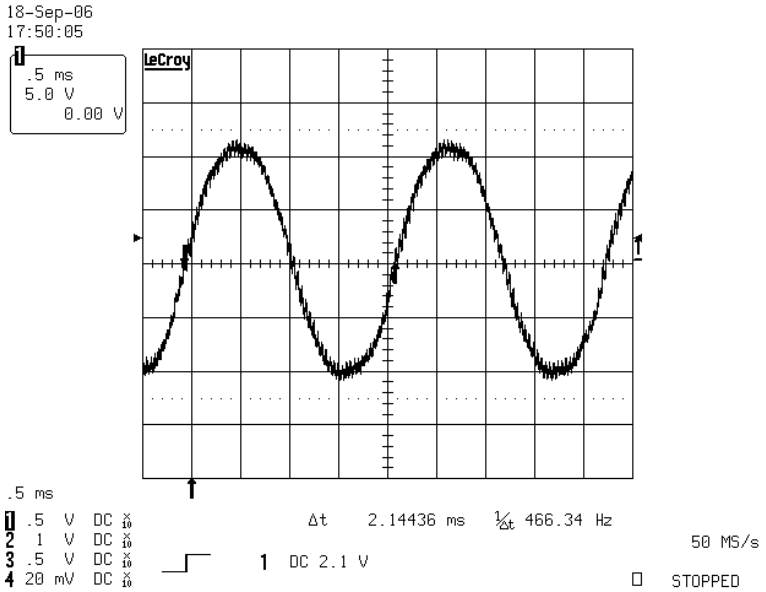

Atmel Corporation

2325 Orchard Parkway
San Jose, CA 95131, USA
Tel: 1(408) 441-0311
Fax: 1(408) 487-2600

Regional Headquarters

Europe
Atmel Sarl
Route des Arsenaux 41
Case Postale 80
CH-1705 Fribourg
Switzerland
Tel: (41) 26-426-5555
Fax: (41) 26-426-5500

Asia
Room 1219
Chinachem Golden Plaza
77 Mody Road Tsimshatsui
East Kowloon
Hong Kong
Tel: (852) 2721-9778
Fax: (852) 2722-1369

Japan
9F, Tonetsu Shinkawa Bldg.
1-24-8 Shinkawa
Chuo-ku, Tokyo 104-0033
Japan
Tel: (81) 3-3523-3551
Fax: (81) 3-3523-7581

Atmel Operations

Memory
2325 Orchard Parkway
San Jose, CA 95131, USA
Tel: 1(408) 441-0311
Fax: 1(408) 436-4314

Microcontrollers
2325 Orchard Parkway
San Jose, CA 95131, USA
Tel: 1(408) 441-0311
Fax: 1(408) 436-4314

La Chantrerie
BP 70602
44306 Nantes Cedex 3, France
Tel: (33) 2-40-18-18-18
Fax: (33) 2-40-18-19-60

ASIC/ASSP/Smart Cards
Zone Industrielle
13106 Rousset Cedex, France
Tel: (33) 4-42-53-60-00
Fax: (33) 4-42-53-60-01

1150 East Cheyenne Mtn. Blvd.
Colorado Springs, CO 80906, USA
Tel: 1(719) 576-3300
Fax: 1(719) 540-1759

Scottish Enterprise Technology Park
Maxwell Building
East Kilbride G75 0QR, Scotland
Tel: (44) 1355-803-000
Fax: (44) 1355-242-743

RF/Automotive
Theresienstrasse 2
Postfach 3535
74025 Heilbronn, Germany
Tel: (49) 71-31-67-0
Fax: (49) 71-31-67-2340

1150 East Cheyenne Mtn. Blvd.
Colorado Springs, CO 80906, USA
Tel: 1(719) 576-3300
Fax: 1(719) 540-1759

Biometrics/Imaging/Hi-Rel MPU/
High Speed Converters/RF Datacom
Avenue de Rochepleine
BP 123
38521 Saint-Egreve Cedex, France
Tel: (33) 4-76-58-30-00
Fax: (33) 4-76-58-34-80

Literature Requests
www.atmel.com/literature

Printed on recycled paper.

7671A–AVR–09/06